To appear in Astrophysical Journal

A Systematic Search for Corotating Interaction Regions in Apparently Single Galactic WR Stars: I. Characterizing the Variability.

N. St-Louis

Département de Physique, Université de Montréal, C.P. 6128, Succ. Centre-Ville, Montréal, Québec, Canada H3C 3J7

stlouis@astro.umontreal.ca

A.-N. Chené

Canadian Gemini Office, Herzberg Institute of Astrophysics, 5071, West Saanich Road, Victoria (BC), Canada V9E 2E7

andre-nicolas.chene@nrc-cnrc.gc.ca

O. Schnurr

Department of Physics & Astronomy, University of Sheffield, Hicks Building, Hounsfield Rd, Sheffield, S3 7RH, UK

o.schnurr@sheffield.ac.uk

and

M.-H. Nicol

Max Planck Institute for Astronomy, Konigstuhl 17, D-69117, Heidelberg, Germany

nicol@mpia.de

ABSTRACT

We present the results of a systematic search for large-scale spectroscopic variability in apparently single Wolf-Rayet stars brighter than $v \sim 12.5$. In this first paper we characterize the various forms of variability detected and distinguish several separate groups. For each star in our sample, we obtained

4–5 high-resolution spectra with a signal-to-noise ratio ~ 100. Our ultimate goal is to identify new candidates presenting variability that potentially comes from Co-rotating Interaction Regions (CIR).

Out of a sample of 25 stars, 10 were found to display large-scale changes of which 4 are of CIR-type (WR 1, WR 115 WR 120 and WR 134). The star WR 134 was already known to show such changes from previous studies. Three WN8 stars present a different type of large-scale variability and we believe deserve a group of their own. Also, all three WC9d stars in our sample present large-scale variability, but it remains to be checked if these are binaries, as many dust-making WR stars are double. Finally, of the remaining stars, 10 were found to show small-amplitude spectral changes which we attribute to normal line-profile variability due to inhomogeneities in the wind, and 5 were found to show no spectral variability, as far as can be concluded from the data in hand.

Follow-up studies are required to identify potential periods for our candidates showing CIR-type changes and eventually estimate a rotation rate for these WR stars.

Subject headings: stars: Wolf-Rayet — stars: variables — stars: winds, outflows — stars: mass-loss

1. Rotation and Spectroscopic Variability of Single Wolf-Rayet Stars

Stellar rotation has now been fully incorporated into evolutionary models of massive stars (eg. Meynet & Maeder 2000; Heger, Langer & Woosley 2000), prompted by several observational facts that were unexplained by previous models without rotation (eg. Meynet et al. 1994; Woosley, Langer & Weaver 1993) and that pointed to a solution related to mixing. For example, Herrero et al. (1992) had found that many O stars, and in particular fast rotators, show an enhanced He abundance; they called this the *helium discrepancy*. The models including rotation have been very successful in reproducing the observed abundances, predicting higher He and N abundances for higher masses and higher rotation velocities. Evolutionary models with rotation have also provided a solution for many other previously unexplained observations such as the well-known blue-to-red supergiant ratio (B/R) problem (e.g. Langer & Maeder 1995). Indeed, when neglecting rotation, evolutionary models were unable to reproduce the rapid increase in B/R with increasing metallicity. As the new models predict many more red supergiants at low metallicity coupled with a shorter blue supergiant phase, they provided a natural solution.

It is now clear that rotation is an important factor in our understanding of massive stars

and their evolution. It is therefore interesting to compare theoretical predictions with the available observational data. For O stars, the latest homogenous, large-scale surveys of projected rotational velocities have been carried out by Penny (1996) and Howarth et al. (1997), who respectively studied 177 and 373 stars, the latter also including early-type B stars. These studies were both based on high-resolution IUE spectra and used a cross-correlation technique with a narrow-line template spectrum to measure the rotational speeds. Both studies note the absence of very narrow lines for supergiants while some smaller velocities are found for main-sequence stars. Instead of interpreting this as a possible increase in rotational velocities as the star evolves, these authors favour an additional broadening mechanism such as macro-turbulence. In fact, Howarth (2004) strengthens this assertion by pointing out that the shape of the absorption lines expected from pure rotation is a poor match to the observed profiles and that a line dominated by transverse turbulence is a much better match. Ignoring this possible effect (most likely small) of macro-turbulence on the projected rotational velocities, their distribution peaks at ~ 80 km s^{-1} and has a very extended high-velocity tail reaching to 400 km s^{-1}. These values are not incompatible with model predictions; on the main sequence, the models show that even if the star starts out with a relatively flat internal rotation profile, the rotation becomes increasingly differential (but never more than a factor of two in velocity) because the convective core is contracting and therefore spinning up, while the outer layers are expanding and therefore slowing down. In spite of this, there is a global decrease in the rotation rate as a function of time as angular momentum is lost through mass-loss. So, depending on their age and their initial rotation rate, the observed velocities are quite acceptable. Interestingly, Penny (1996) notes that, in fact, the higher rotational velocities are generally associated with lower-mass stars. This is an important result. Indeed Meynet & Maeder (2000) predict that the rotation rates decrease more rapidly for higher initial rotation rates and for higher mass and therefore higher mass-loss rate stars, in view of the increased loss of angular momentum. This agrees very nicely with the observations.

For WR stars, very slow average surface rotation velocities in the range 20–70 km s^{-1} are predicted for the He-burning phase, depending on the initial rotation velocity on the main sequence and on the evolutionary state of the star (Meynet & Maeder 2003). The reason for these low values and the narrowness of this range is simple; the amount of mass that must be removed from massive O stars to turn them into WR stars is so big that most of the angular momentum is lost in the process. However, the differential rotation that steadily increased on the main sequence suddenly becomes very pronounced, as the helium core contracts at the end of core hydrogen burning. The star ends up with a core spinning faster than the initial ZAMS rotation velocity.

A fast-spinning core, at least in some WR stars, would support the presently favoured model to explain long-soft Gamma-Ray Bursts (GRBs). Indeed, the so-called *collapsar* model

(Woosley 1993; MacFadyen & Woosley 1999; MacFadyen, Woosley & Heger 2001) involves the collapse of a rapidly rotating massive star in its pre-supernova phase. In this model, the central core becomes a black hole surrounded by a disk. The accretion of matter through the disk creates powerful jets in which the matter travels at very high speeds. Heger & Langer (2000) and Hirschi, Meynet & Maeder (2004), have followed the evolution of a rotating He core to determine if the very rapid core velocities required by the collapsar model could be reached in spite of the many modes of transport and redistribution of the angular momentum taking place (mass-loss, shear, turbulence, convection, etc). They found that indeed this is possible for initial rotation speeds on the main sequence that are typical of that of O stars.

However, adding magnetic fields to the models has brought new elements to the problem. Indeed, Heger et al. (2005) have shown that including magnetic torques caused by a Spruit-Tayler dynamo (Spruit 2002) dramaticaly reduces the angular momentum of the core leading to periods in the resulting pulsar of 15 ms at birth, which is compatible with the average value for common pulsars but much too small to make a long-soft gamma-ray burst (GRB).

Nevertheless, for a rotating star, efficient chemical mixing can occur and if the mixing timescale is shorter than the thermonuclear timescale, the star can remain quasi-chemically homogeneous (Maeder 1987; Langer 1992). In that case, the star lacks the stratified layers which are required for the development of the Spruit-Tayler dynamo (Spruit 2002). This lack of a core-envelope structure prevents the magnetic core-envelope coupling described above and the spin-down of the star's core can be avoided. Woosley & Heger (2006) have shown that for a rapidly-rotating star on the main sequence and if the mass-loss in the WR phase is reduced by a factor of ten, massive-star evolution can indeed lead to a core with sufficient angular momentum to produce a long-soft GRB. The necessary reduced mass-loss in the WR phase favors low metallicity environments for GRBs. Finally Yoon et al. (2006) calculated evolutionary grids for massive stars including rotation and the effects of a Spruit-Tayler dynamo for different metalicities. Still adopting WR mass-loss rates reduced by a factor of ten, they predict that the production of long GRBs should be limited to metalicities smaller than $Z \sim 0.004$. This translates into a peak at a redshift of z=4.

No reliable direct observation of WR rotation rates has ever been obtained. Attempts have been made to estimate them based on the width of (what the authors had assumed to be) photospheric absorption lines in WR spectra (Massey 1980; Massey & Conti 1981), but these have been seriously questioned, as wind expansion and turbulence have not been taken into account.

It may be virtually impossible to obtain the rotationnal velocity of WR stars directly through photospheric line-profiles but it could still be possible to deduce it from periodic variability in photometry or of spectral lines formed in the winds. Indeed, the winds of massive

stars have been demonstrated to be highly variable. In particular, one type of structure in the wind that accounts for some of these variations, Co-rotating Interaction Regions (CIRs), are thought to be closely linked to the rotation of the star. Indeed, these structures are caused by perturbations at the base of the wind that propagate through it and are carried by rotation. This generates a spiral-like structure in the density distribution, analogous to those commonly observed in the solar corona (Hundhausen 1972), which very likely leads to the ubiquitous Discrete Absorption Components in the spectra of O stars (Cranmer & Owocki 1996). These are rarely observed in WR P Cygni profiles as their absorption components are usually saturated (one exception is WR 24; Prinja & Smith 1992). However, it is believed that they also lead to a very characteristic, large-scale, periodic variability pattern in WR-wind emission lines. Dessart & Chesneau (2002) show the unambiguous S-shape pattern in time-series of model spectra of WR emission lines produced as a consequence of these variations. Observational support has been obtained for this type of variability in two clear cases through repeated spectroscopic observations. WR 6 (St-Louis et al. 1995; Morel et al. 1997, P=3.76 days) and WR 134 (McCandliss et al. 1994; Morel et al. 1999, P=2.25 days) show periodic variations without any indication of a companion. The correspondence between the data and models is striking when one considers that optical depth effects, which are certainly occurring in the observed data, have not been included in the models. This brings strong support to the idea that CIRs do in fact trace the **rotation rate** of the star at the base of the wind. According to Hamann et al. (1988, 1995), these stars both have $R_* \simeq 3R_\odot$. This radius corresponds by definition to a Rosseland optical depth of 20. Assuming that CIRs form at this radius, the equatorial rotation speed (at R_*) is ~ 40 km s^{-1} for WR 6 and ~ 70 km s^{-1} for WR 134, not too different from values predicted by evolutionary models. The periods and variability patterns were found to be the same for lines formed at various distances in the wind, indicating that the CIRs are governed by angular momentum conservation which results in a coherent structure in the wind. The period therefore provides a direct measurement of the rotation *rate* of the underlying star. To calculate the rotation velocity we need to know at what radius the perturbation leading to the CIR originates. If this radius is known, we can then calculate the rotation velocity *at that radius*. Much more observations and analysis of variability associated with CIRs are required to reach this goal. Therefore, the above velocities are only given as rough estimates for illustrative purposes.

In an attempt to identify more WR stars displaying CIR-type variability, we have carried out a survey of all Galactic WR stars brighter than $v \sim 12.5$. Our complete sample includes 39 southern stars, which will be discussed in Chené & St-Louis (2009a), and 25 northern stars, which we discuss here. The goal of this paper is to present the different types of spectroscopic variability found in our magnitude-limited sample of stars in a qualitative but also quantitative manner. Our aim is to use these characteristics to establish some guidelines

to help identify the spectroscopic variations associated with CIRs. Once identified, these stars can then be observed more intensively and, if present, periods can be determined. In our second paper, we will build on these basis and use the complete sample to determine the frequency of the various types of line-profile variability. Follow-up papers on individual stars that have been more intensively monitored are also planned.

Our northern sample includes all Galactic WR stars visible from the Mont Mégantic Observatory that are not confirmed as SB1 or SB2 binaries. Our targets are listed in Table 1 where the stars' name, spectral type, RA, DEC and v are provided. When available, we also provide terminal velocities measured either from IUE absorption troughs (Prinja, Barlow & Howarth 1990), from near-infrared line profiles (Howarth & Schmutz 1992) or from optical line profiles (Hamann et al. 2006). The last column indicates each star's variability status (see below). Note that although some stars in our sample have published spectral types that indicate a possible companion (not indicated in the table), none have confirmed orbits. In the case of WR 4 and WR 128, only photometric variations have been found without radial velocity confirmation of binarity. In the case of WR 131, WR 143, WR 156 and WR 158, the claim of binarity is based solely on diluted emission lines (d.e.l.) and/or the presence of absorption lines in the spectrum (+a). However, Hamann & Gräfener (2007) argue that binary status established from the d.e.l or +a criteria is often misleading as WR stars can produce a wide variety of spectra depending on their physical parameters. Those authors have demonstrated that in many cases these types of spectra can be reproduced entirely with a single-star model. In particular, WR 108, WR 156 and WR 158 were among the stars that they reproduced with a single-star model. Our final sample consists of 16 WN stars and 9 WC stars. We have included WR 134 for comparison even though it is already known to show variability thought to be associated with CIRs. However, we have excluded WR 157 because it is too close on the sky to another star that is only $\sim$1 magnitude fainter. The separation between the two stars is $\sim$2.2″, i.e. a value comparable with the average seeing at the mont Mégantic Observatory, where our data were obtained. It was therefore impossible to isolate the WR star in our 1.5″ spectrograph slit.

2. Observations

Our observations were obtained at the 1.6m telescope of the mont Mégantic Observatory in Québec, Canada during 6 runs in 2001 and 2002. Details are given in Table 2 in which the run number, the dates of observations and the Julian Dates (JD) are listed. We used a 830.8 l/mm grating giving a resolution of $\Delta\lambda$=1.6 Å (3 pix.) combined with a 2048×4096 EEV CCD.

Table 1. Our Sample of Single WR Stars in the Northern Hemisphere

Name	Spectral Type[1]	RA (2000)	DEC (2000)	v	v_∞(km s^{-1})			Variability
WR1	WN4	00 43 28.4	+64 45 35.4	10.51	2100[3]	1900[4]		LSV
WR2	WN2	01 05 23.03	+60 25 18.9	11.33	3200[3]	1800[4]		NV
WR3	WN3	01 38 55.63	+58 09 22.7	10.70		2700[4]		SSV
WR4	WC5	02 41 11.68	+56 43 49.7	10.53				NV
WR5	WC6	02 52 11.66	+56 56 07.1	11.02				NV
WR106	WC9d	18 04 43.66	-21 09 30.7	12.33				LSV
WR108	WN9h	18 05 25.74	-23 00 20.3	10.16	1220[3]	1170[4]		SSV
WR110	WN5-6	18 07 56.96	-19 23 56.8	10.30	3190[3]	2300[4]		SSV
WR111	WC5	18 08 28.47	-21 15 11.2	8.23	2415[2]	2300[3]		NV
WR115	WN6	18 25 30.01	-14 38 40.9	12.32	1480[3]	1280[4]		LSV
WR119	WC9d	18 39 17.91	-10 05 31.1	12.41				LSV
WR120	WN7	18 41 00.88	-04 26 14.3	12.30	1225[3]	1225[4]		LSV
WR121	WC9d	18 44 13.15	-03 47 57.8	12.41	1300[3]			LSV
WR123	WN8	19 03 59.02	-04 19 01.9	11.26	970[4]			LSV
WR124	WN8h	19 11 30.88	+16 51 38.2	11.58	710[4]			LSV
WR128	WN4(h)	19 48 32.20	+18 12 03.7	10.54	2270[2]	2050[4]		SSV
WR131	WN7h	20 00 19.12	+33 15 51.1	12.36	1400[4]			SSV
WR134	WN6	20 10 14.20	+36 10 35.1	8.23	1905[2]	1960[3]	1700[4]	LSV
WR135	WC8	20 11 53.53	+36 11 50.6	8.36	1405[2]	1500[3]		SSV
WR136	WN6(h)	20 12 06.55	+38 21 17.8	7.65	1605[2]	1760[3]	1600[4]	SSV
WR143	WC4	20 28 22.68	+38 37 18.9	11.95				SSV
WR152	WN3(h)	22 16 24.05	+55 37 37.2	11.67	1800[3]	2000[4]		SSV
WR154	WC6	22 27 17.82	+56 15 11.8	11.54	2700[3]			NV
WR156	WN8h	23 00 10.13	+60 55 38.4	11.09	660[4]			LSV
WR158	WN7h	23 43 30.60	+61 55 48.1	11.46	900[4]			SSV

[1]Spectral types are from van der Hucht (2001)

[2]Prinja, Barlow & Howarth (1990)

[4]Howarth & Schmutz (1992)

[4]Hamann et al. (2006)

Table 2: Observing Runs

Observing run No.	Dates	Julian Date
1	25/06/2001–05/07/2001	2452086–2452096
2	26/07/2001–02/08/2001	2452117–2452124
3	01/10/2001–07/10/2001	2452184–2452190
4	19/06/2002–24/06/2001	2452445–2452450
5	17/07/2002–26/07/2002	2452473–2452482
6	16/10/2002–24/10/2002	2452564–2452572

Our goal is to identify new large-scale variability within our sample of stars. The extra features we are looking for on top of the main emission lines are quite large and therefore easy to find. Based on our previous experience with WR 6 and WR 134, we have made the assumption that a small number of good quality spectra, well sampled in time are sufficient to identify new candidates showing variability possibly associated with CIRs. Of course, to quantify the changes and determine the period, a more thorough follow-up will subsequently be required. Therefore, we set out to obtain 4–5 spectra per star in our sample.

The spectra were reduced using the IRAF software package in the standard way. First a bias was subtracted, then each image was divided by a flat field. After extracting the spectra, the wavelength calibration was carried out using a He-Ar calibration lamp. Although our original spectral range was 1500 Å wide, we were forced to reject the reddest part of the spectrum due to a lack of usable lines in the calibration spectra. The final wavelength interval is $\Delta\lambda$=4500-5200 Å. The signal-to-noise ratio of the spectra ranges from 100 to 120.

As our spectra are not photometrically calibrated, the final step of our data reduction procedure was to rectify the spectra. To do so, we have fitted a low order Legendre polynomial to wavelength regions with no strong spectral lines and divided our spectra by the fitted curves.

3. Variability Search

The final spectra are shown in the top panels of Figures 1 to 13 for the two strongest lines present in our wavelength interval. For WN stars these are HeIIλ4686 and HeIIλ4860 while for WC stars they are CIIIλ4650 and CIVλ5016. For each star we plot the differences between individual spectra and the global mean (which is shown in the second panel from

the top). The differences have been shifted vertically for clarity. The Heliocentric Julian Date (HJD) of each observation is indicated on the left-hand side of the plot and the scale factor of the ordinate is indicated in the top right-hand corner of each panel. The graphs are organised by spectral type starting with WN stars from early to late types (Figures 1 to 8) followed by WC stars from early to late types (Figures 9 to 13). Note that for WR 4, WR 111, WR 5 and WR 154, we do not show the plot of the CIIIλ4650 line because in those cases the line was on the extreme edge of the wavelength interval and therefore there was not enough continuum on one side of the line to allow for an accurate enough spectrum rectification. This could lead to a false detection of line variability. We prefer to adopt a conservative approach in this respect.

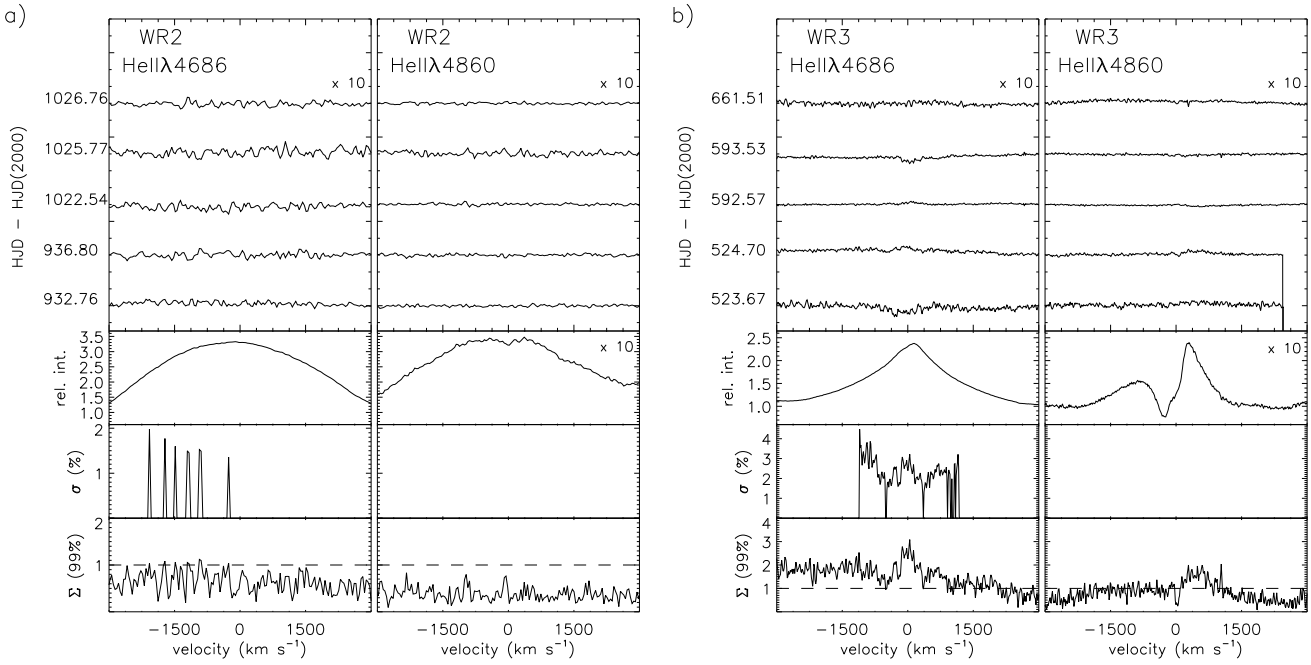

Fig. 1.— a) *top*: Montage of the HeIIλ4686 (left) and HeIλ4860 (right) residuals (individual spectra − mean) for WR 2 (WN2). For both cases, the scale factor of the ordinate is indicated in the top right-hand corner of the plot. HJD - HJD(2000) is indicated in the y-axis. *second from top*: Mean spectrum. *second from bottom*: σ-spectrum. *bottom*: Σ (99%) spectrum. b) The same as a) for WR 3 (WN3ha).

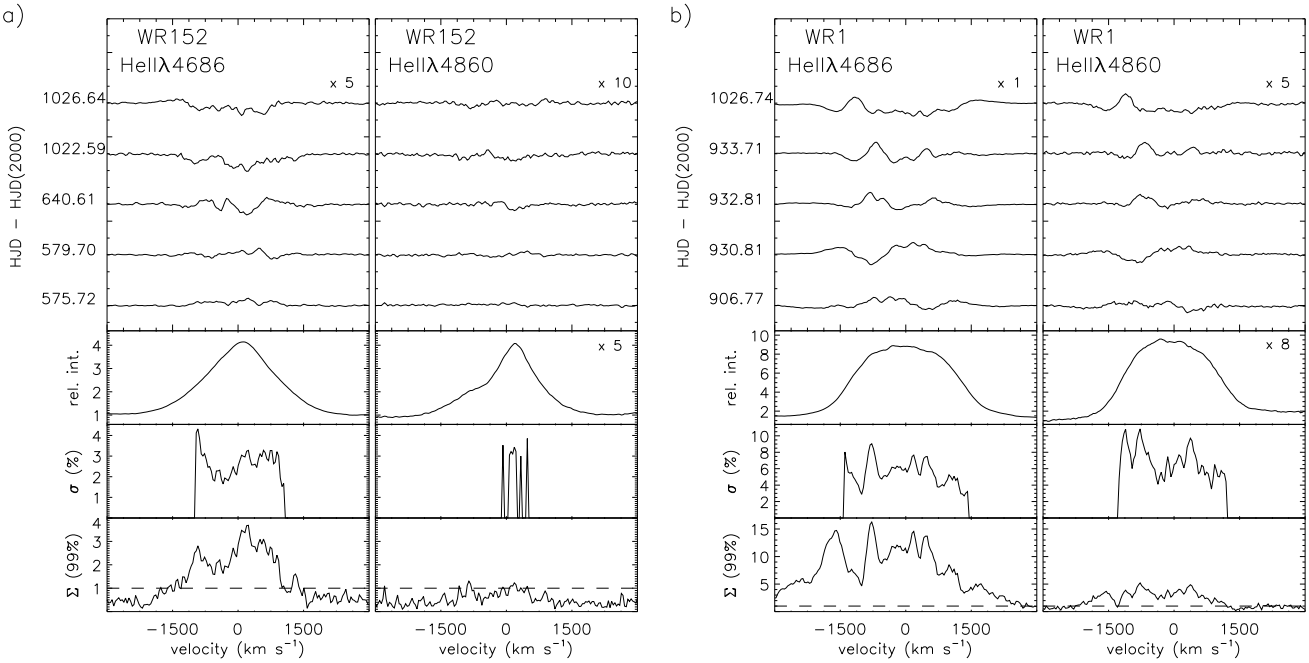

Fig. 2.— Same as Fig.1 for a) WR 152 (WN3) and b) WR 1 (WN4).

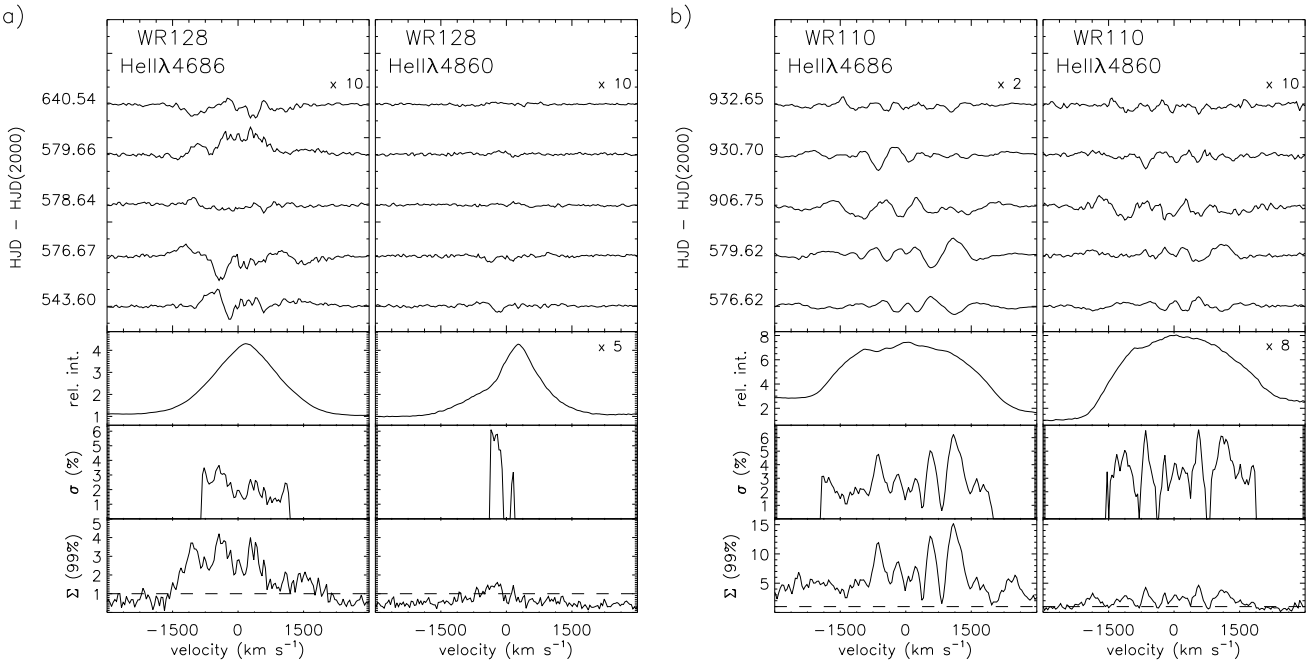

Fig. 3.— Same as Fig.1 for a) WR 128 (WN4(h)) and b) WR 110 (WN5–6).

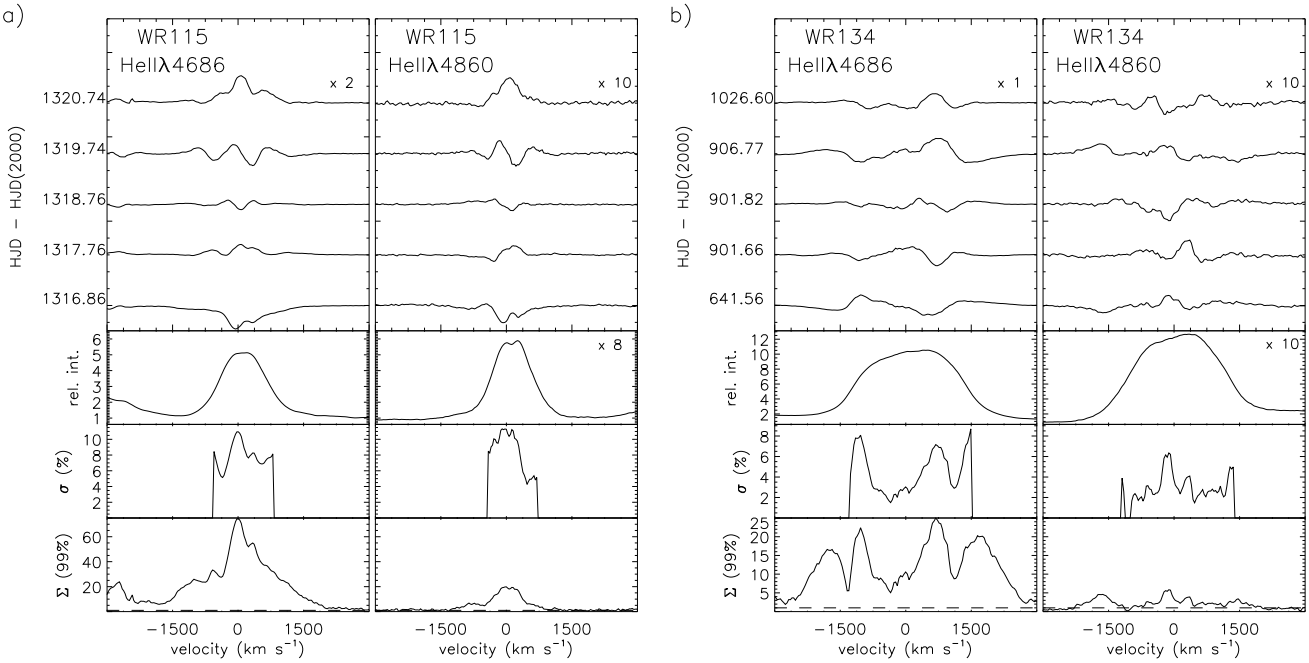

Fig. 4.— Same as Fig.1 for a) WR 115 (WN6) and b) WR 134 (WN6).

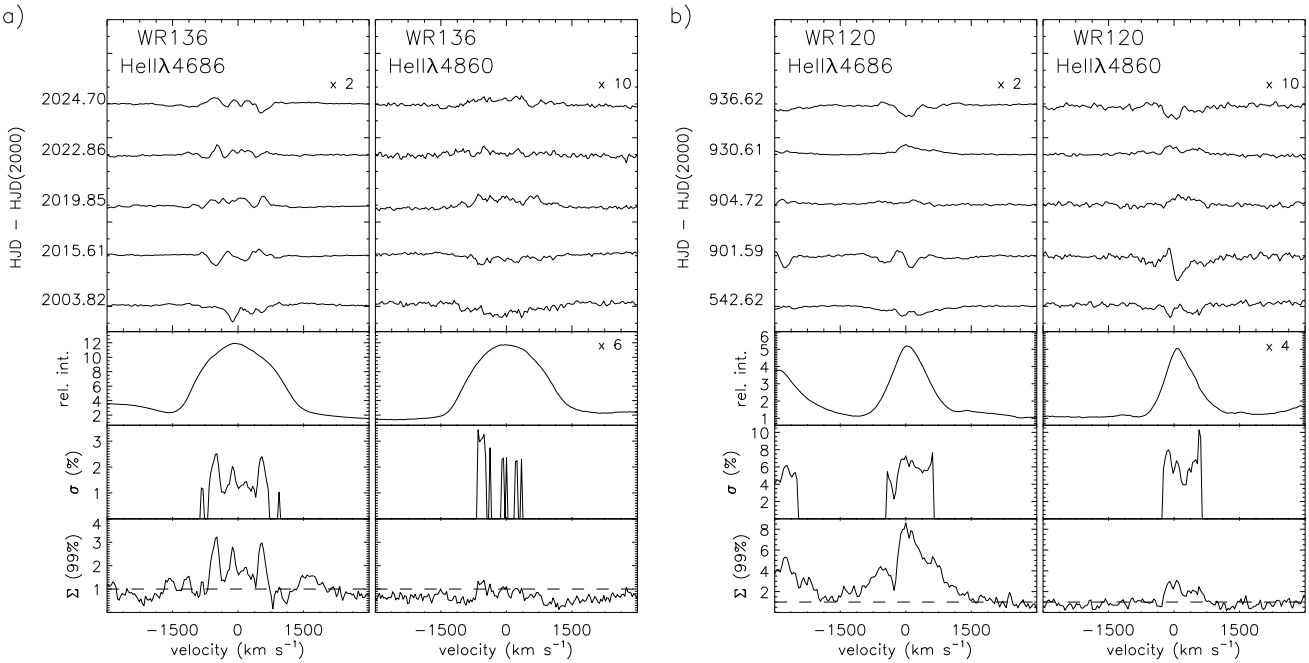

Fig. 5.— Same as Fig.1 for a) WR 136 (WN6) and b) WR 120 (WN7).

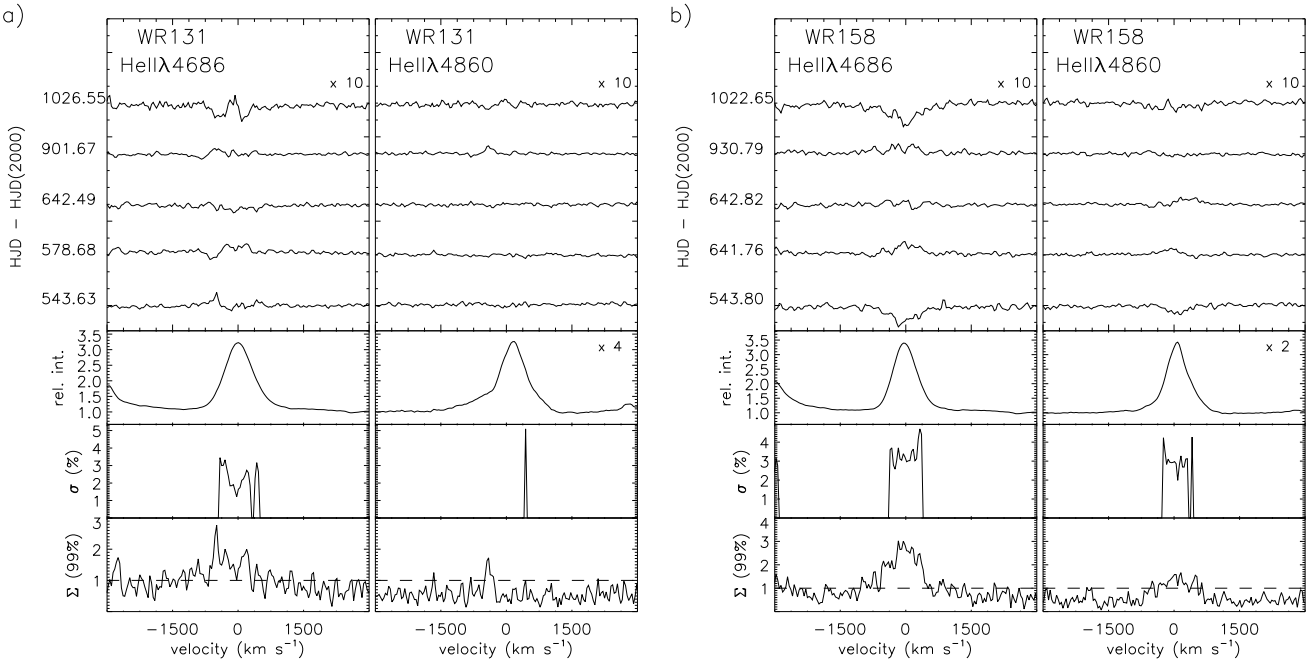

Fig. 6.— Same as Fig.1 for a) WR 131 (WN7h) and WR 158 (WN7h).

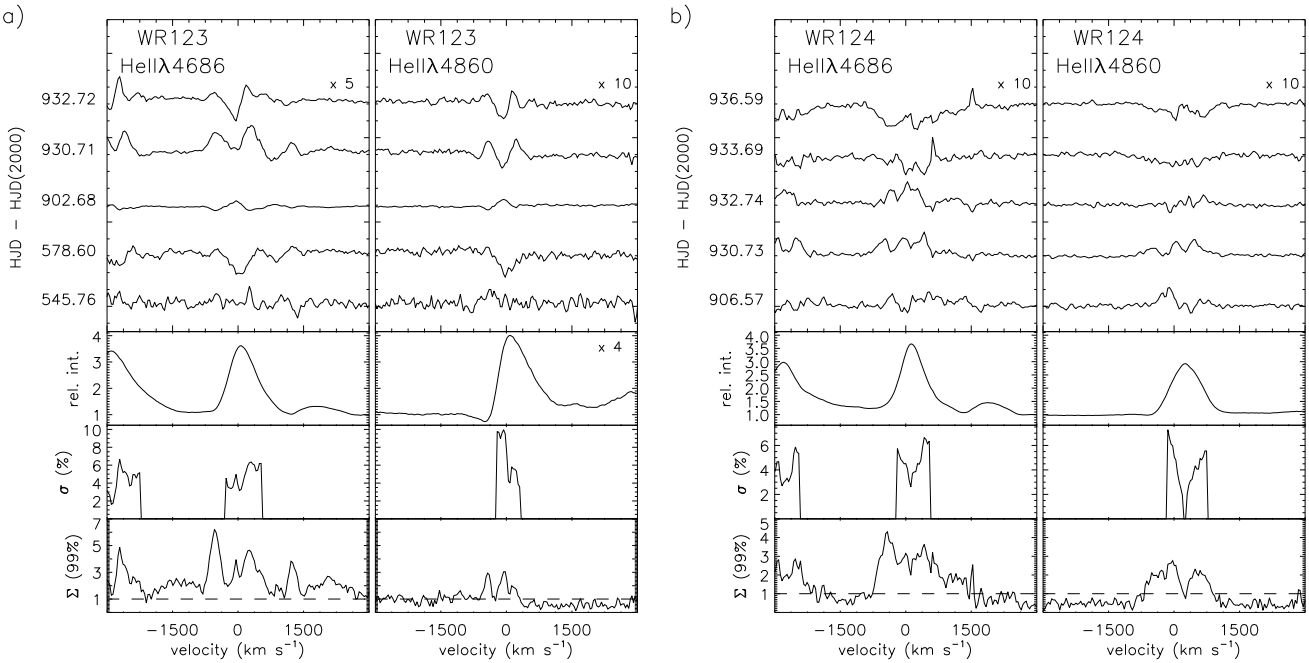

Fig. 7.— Same as Fig.1 for a) WR 123 (WN8) and b) WR 124 (WN8h).

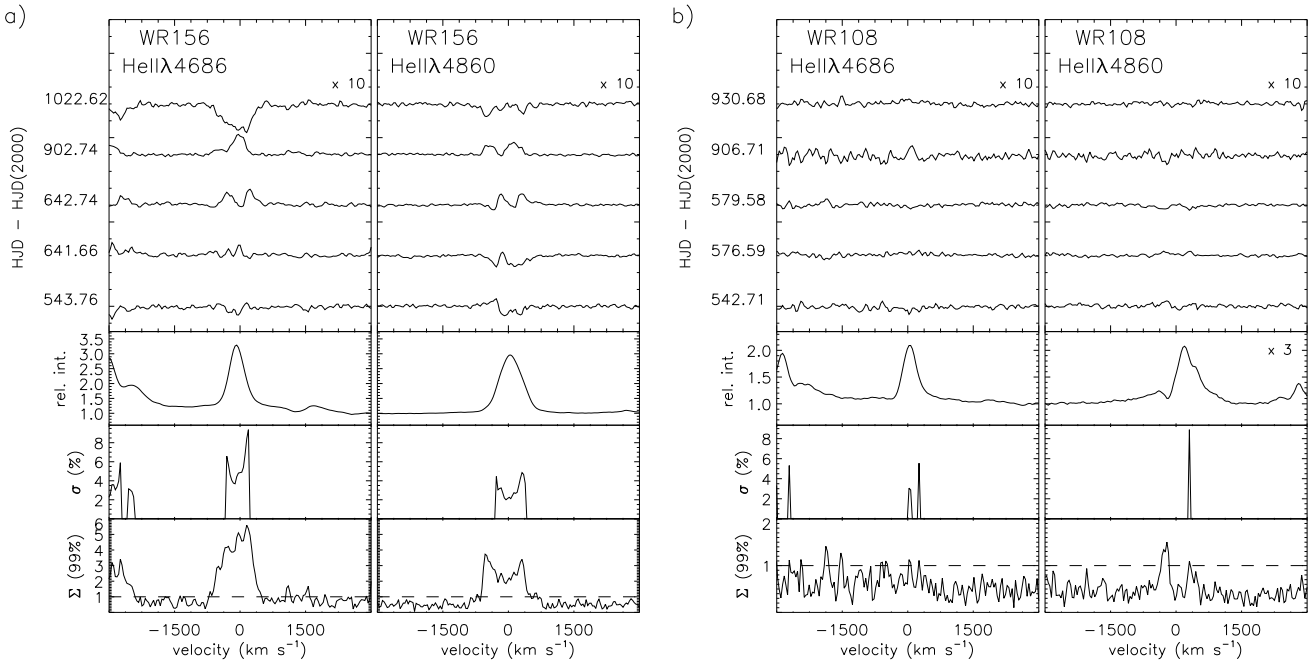

Fig. 8.— Same as Fig.1 for a) WR 156 (WN8h) and b) WR 108 (WN9h).

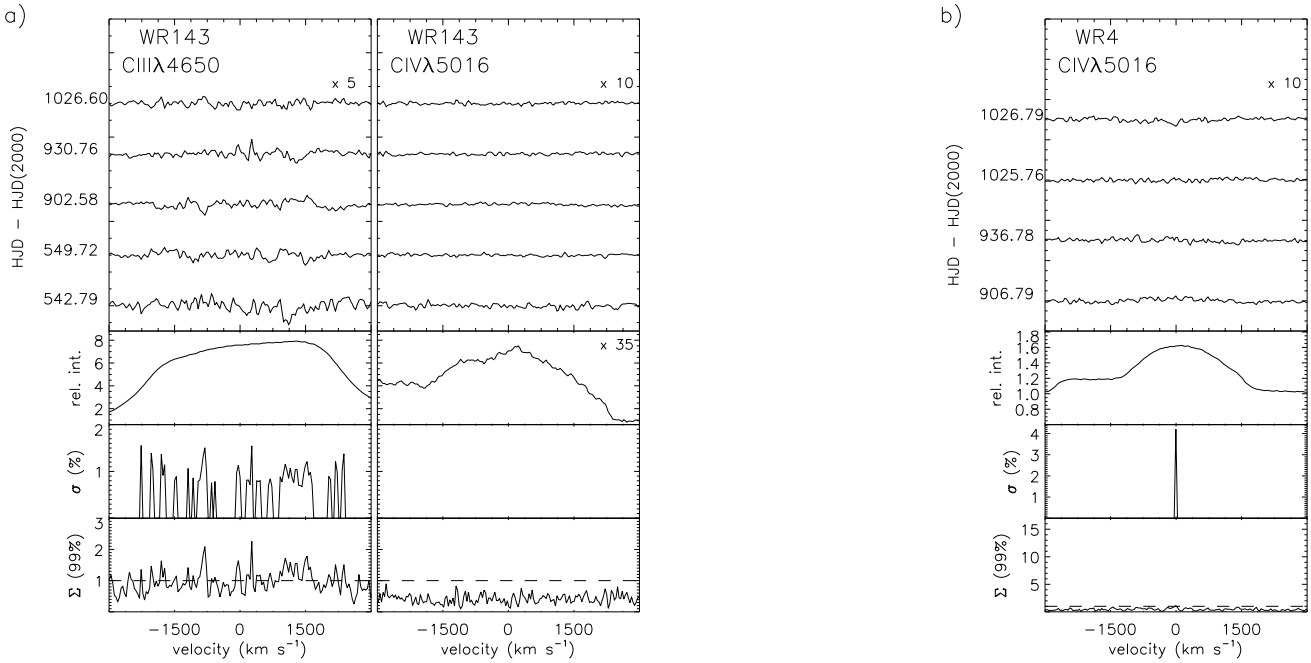

Fig. 9.— Same as Fig.1 for a) WR 143 (WC4) and b) WR 4 (WC5) for the CIIIλ4650 (left) and CIVλ5016 (right) line-profiles. Note that for WR 4, the montage for the CIIIλ4650 line is not shown as the data are unusable.

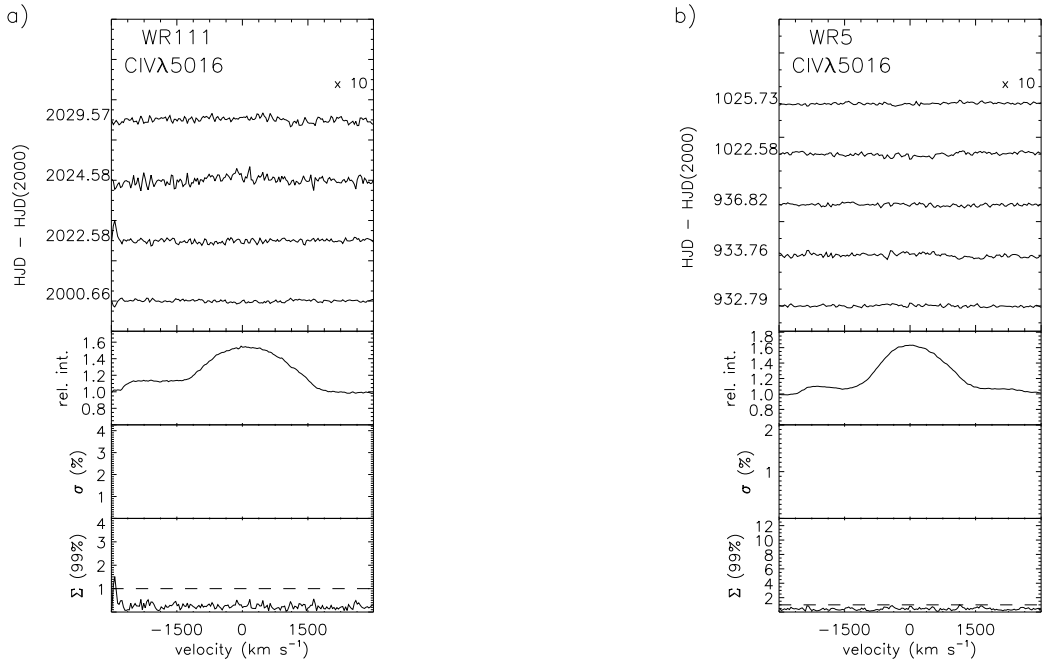

Fig. 10.— Same as Fig.9 for a) WR 111 (WC5) and b) WR 5 (WC6). Note that the montage for the CIIIλ4650 line is not shown as the data are unusable.

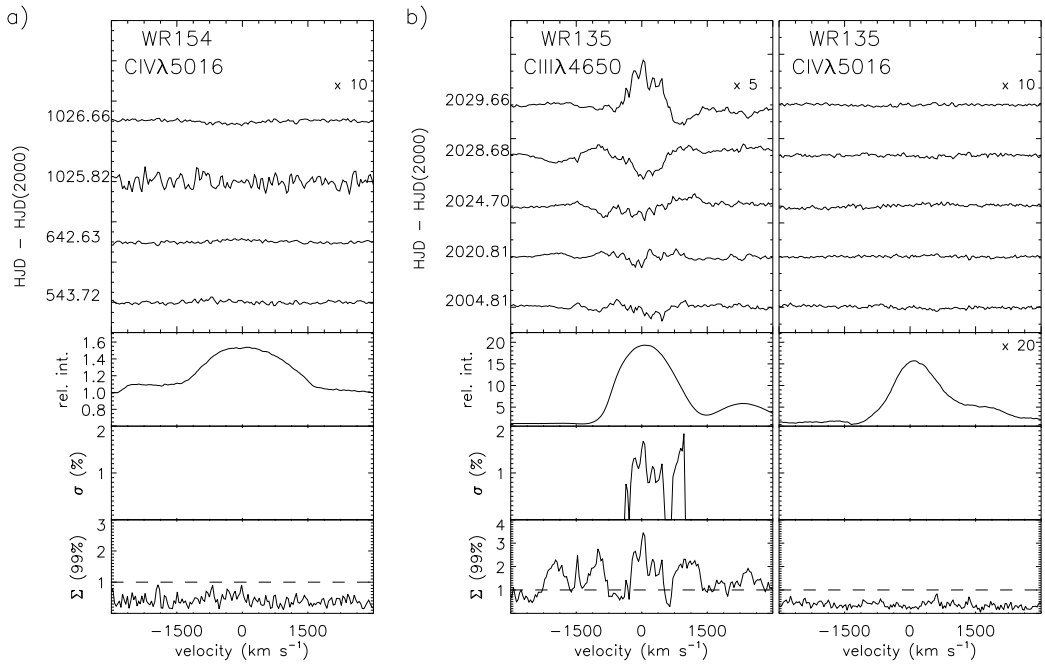

Fig. 11.— Same as Fig.9 for a) WR 154 (WC6) and b) WR 135 (WC8). Note that for WR 154, the montage for the CIIIλ4650 line is not shown as the data are unusable.

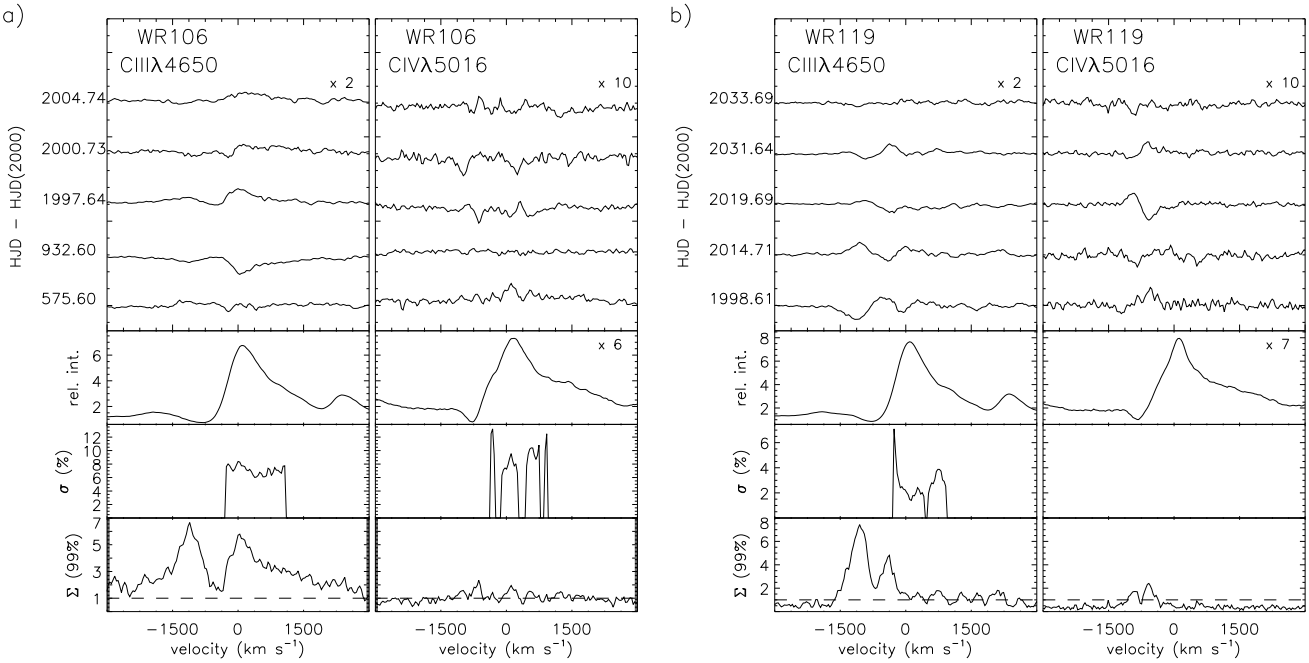

Fig. 12.— Same as Fig.9 for a) WR 106 (WC9d) and b) WR 119 (WC9d).

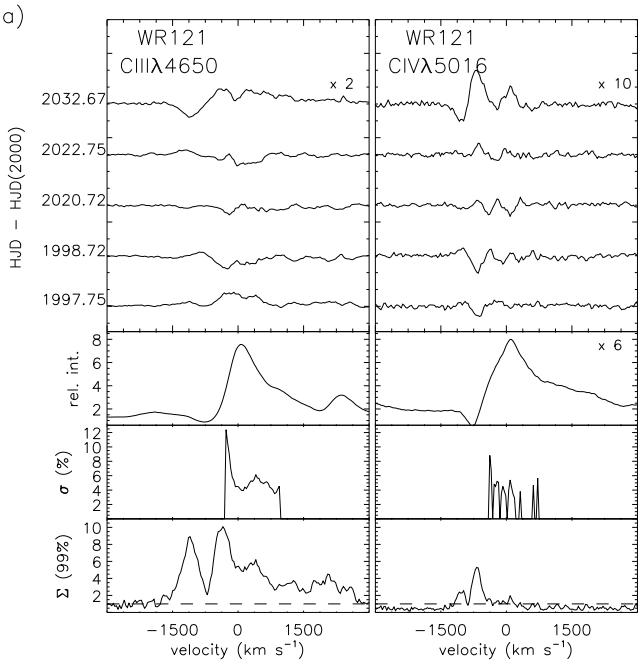

Fig. 13.— Same as Fig.9 for WR 121 (WC9d).

In order to search for significant spectroscopic variability among our targets, we have adopted the formalism of Fullerton et al. (1996). First, we have calculated the temporal variance spectrum (TVS), which is a statistically rigorous means of identifying the variable parts of our spectra. For N spectra, the TVS at wavelength j is defined by:

$$(TVS)_j = \frac{1}{(N-1)} \sum_{i=1}^{N} \frac{w_i}{\alpha_{ij}} (S_{ij} - \bar{S}_j)^2, \tag{1}$$

where the weights of the individual spectra, w_i, are given by $w_i = (\frac{\sigma_0}{\sigma_{ic}})^2$ with

$$\sigma_0{}^2 = \left(\frac{1}{N} \sum_{i=1}^{N} \sigma_{ic}{}^{-2} \right)^{-1},$$

a standardized dispersion. Here, $\bar{S}_j$ is the weighted mean spectrum, σ_{ic} is the noise in the continuum and α_{ij} are wavelength correction factors given by $\alpha_{ij} = (\frac{\sigma_{ij}}{\sigma_{ic}})^2$, σ_{ij} being the noise associated with the flux S_{ij}.

Then, we have established the level of significant variability assuming that our data are governed by a reduced chi-squared distribution with N−1 degrees of freedom. Using the standardized dipersion, σ_0, for scaling, we therefore adopt a threshold of : $\sigma_0^2 \chi^2_{N-1}(99\%)$. Finally, we used $\Sigma_j(99\%) = \sqrt{\frac{(TVS)_j}{\sigma_0^2 \chi^2_{N-1}(99\%)}}$ to quantify the level of variability at each wavelength: a spectrum that reaches a level of 1, is variable at a 1 σ level, if it reaches 3 it is variable at a 3 σ level, etc. We have chosen a confidence level of 99%, which means that if the value of $\Sigma_j(99\%)$ reaches 3, we are 99% confident that the spectrum is variable at a 3 σ level. We note that as the standardized dispersion, σ_0 is calculated using the noise level in the continuum regions and as the spectra are rectified, there is no real information on the variability of the continuum regions. In the bottom panels of Figures 1 to 13, we have plotted the $\Sigma(99\%)$ spectrum for each star for easy comparison with the spectra plotted above.

Inspection of Figures 1 to 13 reveals that the majority of the stars in our sample show significant variability in at least one of the two main spectral lines in their spectrum. One notable exception is the WN2 star WR 2. For WR 4, WR 5, WR 111 and WR 154, we did not detect variability in the weak CIV line, but we only have limited information at our disposal since we do not have usable data in the strong CIII line. It is clear that the level of variability is quite different from one star to another. The variations range from a few σs to close to 60σs in WR 115. As the quality of our spectra is relatively uniform, we can, in principle, compare the σ from star to star, but its value only provides information on the significance of the changes with respect to the noise level of our data.

As the line strengths are very different from star to star, comparing the significance level of the variations does not provide useful physical information. A quantity that is potentially

more interesting is the fraction of the line flux that is variable. To characterize this, it is best to use a quantity that is representative of the variance in pixel j compared to the noise at that wavelength (σ_{ij}) rather than use a weight that is linked to the noise in the associated continuum, as the TVS does. To do this, Chené (2007) has defined a modified TVS as follows:

$$(TVS_{mod})_j = \frac{1}{(N-1)} \sum_{i=1}^{N} \left(\frac{\sigma_{0j}}{\sigma_{ij}} (S_{ij} - \bar{S}_j) \right)^2, \tag{2}$$

where σ_{0j} is the reciprocal of the rms of the signal-to-noise ratio at pixel j of the spectral line series.

In order to quantify what fraction of the line flux (without the contiuum) is variable, we divide this value by the line flux, $(\bar{S}_j - 1)$. Of course this quantity has no meaning outside emission lines and in particular in continuum regions. To avoid any problems, we therefore limited our caculations to a width corresponding to a relative intensity level of 1.3 of each line. Also, for very weak lines (< 1.3 in relative intensity), our ratio becomes meaningless because the line flux, the denominator, is too close to zero and the variability level, the numerator, is dominated by the noise. In such cases, we have left the panel blank. Finally, absorption components of P Cygni profiles are also excluded since in that case the value of $(\bar{S}_j - 1)$ will be negative and cannot be compared directly with what is observed in emission lines.

The values of $\sigma_j = (TVS_{mod})_j^{1/2}/(\bar{S}_j - 1)$ are plotted in the middle panels of Figures 1 to 13. Several interesting conclusions can be drawn from these plots. First, for all types of stars, both lines show roughly the same level of variability. However, one has to note that in the case of WN stars, we compared lines of the same ion and therefore it is likely that in a given star, these two lines are formed in similar regions of the wind. The line widths are indeed, in most cases, very similar. Another interesting feature of the variability is that the calculated values of Σ are much stronger in P Cygni absorption components than in the corresponding emission components, i.e. the variations are more significant. This is perhaps not surprising since that part of the profile comes from a much smaller volume of the wind than the emission and therefore suffers less from cancelling effects from large-scale changes in density or ionisation arising in different parts of the wind. This effect is clearly present in the P Cygni profile of WR 123 (He IIλ4686) or WR119 (C IIIλ4650), for example.

After a careful examination of Figures 1 to 13, we divide our sample in three main categories: stars showing no profile variability (NV), stars showing small-scale profile variability (SSV — $\sigma < 5\%$) and stars showing large-scale variability (LSV — $\sigma > 5\%$). Note that the stars designated as NV are not necessarily stars that do not show spectral variability, but rather that no significant variability can be detected at a level of confidence of 99% on

spectra having signal-to-noise ratio ∼100. Our conclusions are listed in the last column of Table 1. The detected subpeaks have widths that range from ∼140 km s^{-1} for the smallest isolated structures to ∼350 km s^{-1} for the largest. Unfortunately, our limited dataset does not allow us to search for correlations between these widths and, for example, the level of variability or the width of the global line. In the following sections we will discuss in turn the variability we found in WN and WC stars.

3.1. WN Stars

Significant variability has been found in all but one WN star in our sample, i.e. WR 2, the WN star of the earliest type. However, this seems to be an unusual WR star. Hamann et al. (2006) note that this star has unique line-profile shapes. These authors were unable to reproduce its spectrum using their model atmospheres without convolving the normal wind lines with a rotation profile with a velocity of 1900 km s^{-1}, which is very close to the star's critical velocity. This is, of course, a simplistic way of including the effects of rotation on the line profile and is likely to lead to improbable conclusions but it reflects the fact that the line-formation process for this star is not totally understood and that the star is unusual in that respect.

For WR 3, WR 152, WR 128, WR 136, WR 131, WR 158 and WR 108, variability has indeed been detected but at a relatively low level of $\sigma \sim 2-3\%$ of the line flux. The nature of the changes is also very different from the CIR-type variability we first set-out to identify. The structures are small and are most likely stochastic changes associated with inhomogeneities in the wind of WR stars, such as discussed from an observational point of view by Moffat et al. (1988) and Lépine et al. (1996), for example. More recently, there have been some insightful theoretical investigations into small-scale inhomogeneities in the winds of hot stars. Dessart & Owocki (2002a,b, 2003, 2005a,b) present radiation hydrodynamic simulations of hot-star winds line-profile variations that arise as a consequence of the intrinsically unstable nature of the line-driving mechanism of the wind. Those calculations show, for example, that including Rayleigh-Taylor or thin-shell instablities together with some lateral averaging of the diffuse radiation is important to understand the behaviour of the width of the subpeaks as a function of their position on the line profile, i.e. the lateral versus radial size of the small scale inhomogeneities in the wind. We believe that the characteristics of the variations seen in the stars that we classify as SSV, are compatible with the type of changes caused by such small-scale inhomegeneities in the wind.

For WR 1, WR 110, WR 115, WR 134, WR 120, WR 123, WR 124 and WR 156, the variations have a much larger amplitude. Therefore, it is quite likely that the physical

phenomenon from which they originate is different from what is observed for SSV stars. We discuss these stars in more detail below.

WR 134 is well-known to show CIR-type variability for which a period of 2.3 days has been identified (e.g. McCandliss et al. 1994; Morel et al. 1999). We use it as a test that indeed with 4–5 spectra we can identify easily the type of variability we are looking for. One can clearly see on top of both the HeIIλ4686 and HeIIλ4860 lines, broad emission excesses at different positions on the line. The changes are highly significant and reach σ = 6–8 % of the line flux.

Three other WN stars show a similar type of variability: WR 1, WR 115 and WR 120. These stars clearly show CIR-type variations; large-scale structures are seen superposed on the broad emission lines reaching σ $\sim$7–8% of the line flux in WR 1 and WR 120 and σ $\sim$10$-$12% of the line flux in WR 115. We therefore classify these stars as LSV and further put them in the CIR-type category.

The situation is less clear for WR 110. Clear structures can be distinguished on both spectral lines. The variations reach a level of σ $\sim$5% of the line flux, which is significantly higher than the other stars we have classified as SSV and that we associate with small-scale wind inhomogeneities. However, the detected structures are not quite as strong as for those showing variability thought to be associated with CIRs. Therefore, we classify this star as a SSV and use it to establish our approximate upper limit for the level of small-scale/blob-like variability.

Finally, for WR 123, WR 124 and WR 156, all WN8-type stars, a different type of variability is found. The changes reach a relatively high level (from 5 to 10% of the line flux) but appear to be different in nature from those thought to be associated with CIRs. The σ profile has a very typical shape with two maxima, one on the red and the other on the blue side of the emission line and a minimum at line center. The only exception is the HeIIλ4686 profile of WR123 but in that case there is a very strong contrast between the variability in the absorption component and that of the emission. In fact this effect of a more variable absorption component seems to be amplified in WR 108, the only WN9 star in our sample. Indeed, despite the fact that we have classified this star as SSV, the changes are different in nature from that observed in the other stars we have put in that category. In this case, the variability is actually confined to the P Cygni absorption component of the HeIIλ4860 line, which is clearly present. In view of the specific nature of the changes, we create a separate class of LSV for WN8-type stars. Actually, WN8 stars are well-known to display an unusual behaviour. Marchenko et al. (1998) presented a comprehensive study of the photometric and spectroscopic variability patterns of 10 Galactic WN8 stars and found a link between the level of variability in the continuum and in spectral lines which they suggest may be

linked to pulsational instabilities. Other unusual behaviours of WN8 stars as summarized by Marchenko et al. (1998) include a low binary frequency, a high distance from the Galactic plane and/or runaway speeds and the fact that they are rarely found in stellar clusters and associations. Therefore, it is perhaps not surprising to find that they fall in a class of their own compared with other types of WR stars when it comes to spectral variability.

3.2. WC Stars

Because of problems with our spectrum rectification procedure of the CIIIλ4650 lines in our early-type WC stars, the information at our disposal for these stars is more limited than for WN stars. Indeed, this line is located very close to the blue extremity of our wavelength interval. Therefore, the continuum regions that are available bluewards of the line are much more restricted. This reduces the accuracy that can be achieved during the spectrum rectification procedure. Of course, the higher the contrast of the line with respect to the continuum, the more it is affected by this effect. The WC4 star WR 143 has a somewhat weaker CIII line than the other early WC stars and therefore we were able to obtain a sufficiently accurate rectified line profile. Note that this line is slightly affected by blending with the neighbouring HeIIλ4686 line. This is the reason why the line rises towards the red. However, the CIVλ5016 line in that star is practically inexistent. We classify this star as SSV as its variability level is $\sim 1\%$ of the line flux.

For WR 4, WR 111, WR 5 and WR 154, all WC5 and WC6 stars, no variability is detected in the weak CIVλ5016 line, which is the only usable line in our wavelength range. We therefore classify them as stars showing no profile variabilities (NV) but note that new observations of a stronger line should be obtained to verify this assertion.

For WR 135, we find small-scale variability only in the CIIIλ4650 line. The CIVλ5016 line is constant at the level of accuracy of our dataset. This star has been clearly identified as a typical, small-scale variable by Robert (1992) and Lépine et al. (1996). We reach the same conclusion here; we classify it as a SSV.

Finally, the three WC9d stars, WR 106, WR 119 and WR 121, all reach a high level of variability. However, as indicated by their spectral types, these WC stars are thought to produce carbon-based dust in their atmosphere. Some WC dust makers have been shown to be binaries (e.g. the well-known system WR 140; Hackwell et al. 1976; Williams et al. 1978). In that case, it is believed that the dust is produced within the cone-shaped shock formed as a consequence of the collision between the two stellar winds. As the gas flows along the shock cone, it eventually reaches distances where the density compression is still adequate

for dust formation and the intensity of the ultraviolet flux from the star is sufficiently low not to destroy it. For single stars, however, a definite mechanism to form dust in the wind has yet not been identified. Shocks within the wind itself caused by radiative instabilities have been claimed to be possible sources (Zubko 1993a,b). Since all three of our WC9d stars are variable with a large amplitude, we believe that caution must be used, since colliding-wind binaries have been shown to display line-profile variability in the optical with characteristics very similar to that of CIRs (e.g. Hill et al. 2000). It is therefore possible that the WC9d stars in our sample are yet un-identified binaries. We plan to investigate this further by carrying out intensive spectroscopic and photometric monitoring campaigns of these stars. Only a detailed study can reveal if the changes are due to a colliding-wind shock-cone or to CIRs. Therefore, we classify these stars as LSV but create a separate class, the WC-late dust makers.

4. Discussion & Conclusion

The results of our search for optical spectroscopic variability among presumably single WR stars can be summarised as follows. For eight stars, WR 3, WR 152, WR 128, WR 136, WR 131, WR 158, WR 108 and WR 135, variability was found but at a small level compared to the flux of the line. This type of variability is most-likely associated with inhomogeneities in the dense WR wind, which move with it and reveal themselves as small-scale structures superposed on the broad emission lines. In more detailed studies, they have been found to move from line center to the edges of the lines as described for example by Moffat et al. (1988) and Lépine et al. (1996). As the driving mechanism for these radiatively-driven winds has been found to be inherently unstable (Owocki et al. 1988), such variability is expected for all WR stars.

Nevertheless, for 5 other stars in our sample, namely WR 2, WR 4, WR 111, WR 5, WR 154 we found no significant line-profile variability. Note however that in the last 4 cases, our conclusion is based solely on a single relatively weak line. In fact, WR 111, is a star that is known to display small-scale spectral variability due to the presence of inhomogeneities in its wind and has been studied by Lépine & Moffat (1999). In any case, identifying a star as non-variable always depends on the quality of the data in hand. Down to what level of accuracy these stars are constant is, indeed, an important question. One would like to verify if *all* WR stars have inhomogeneities in their winds, if some stars present a different level of variability and if so, what is the cause of this difference. This kind of information can help us better understand the physical mechanisms responsible for these unstable outflows.

Nine stars in our sample presented large-scale profile variability. Of these, we have

identified three new candidates for CIR-type variability: WR 1, WR 115 and WR 120. Follow-up observations with a high temporal resolution will be required to determine if these changes are periodic and if so identify the period. We have done so already for WR 1 and present our results in an upcoming paper (Chené & St-Louis 2009b).

Although the results presented here are not yet for our complete sample, it is interesting to compare our findings to what is known for OB stars. Although the presence of DACs in O-star P Cygni profiles is found to be common (e.g. Howarth & Prinja 1989), cyclical variability in emission lines is not found to show the same ubiquitous behavior. Morel et al. (2004) present a long-term monitoring campaign of the Hα line of 22 bright OB supergiants. Variability was found in all cases with two possible origins: either the underlying photospheric profile and/or a wind component. Cyclical changes which very likely originate from large-scale structures in the wind were found for only two stars in their sample ($\sim$ 14% of the stars). In this study we have identified 4 CIR-type variables (3 of which are new) out of a sample of 25, or $\sim$ 16% , a very similar fraction. Alternatively, we can exclude the WN 8 and WC 9 stars from this estimate; if we do so we also obtain a similar fraction, 4/19$\sim$21%. This striking difference between variability in P Cygni absorption components and emission lines is most likely due to the fact in the former we are sampling a much more physically restricted volume of the wind (i.e. that in front of the star) compared to the entire wind which can be subject to cancelling effects in parts of the wind which are physically distinct but that are travelling at a similar projected velocity.

In addition to the stars showing variability thougt to be associated with CIRs, we have defined two distinct classes of LSV: WN8 stars which are already known to be a peculiar class of WR stars and WC9d stars. In the latter case, it remains to be checked if the changes originate in the wind of a single star because of the presence of CIRs or if these stars are in fact colliding-wind binaries. If of binary origin, a very similar variability pattern is expected with some differences that can be identified with a detailed monitoring campaign. For example, strong epoch-dependancy in spite of the presence of periodic changes would suggest a single-star origin. Also, shock-cones translate into a very distinct and easily recognisable variability pattern on spectral lines, translating to at most, two large excess emissions moving around periodically on the emission line.

Although our survey has revealed a relatively small fraction ($\sim$12%) of stars showing line-profile variability thought to be associated with CIRs among WR stars, it still provides some new candidates for potential estimates of WR rotation velocities. It also provides us with the opportunity to study in more detail the CIR phenomenon for which still very little is known by providing a larger pool of candidates to observe. It is clear that better observational constraints of this phenomenon are crucial to reach a greater understanding of

the physical mecanisms from which they originate.

We wish to thank G. Skalkowsky, C. Foellmi and G. Caron for participating in observing campaigns in 2001/2002. We are also grateful to the (anonymous) referee for comments that led to an improvement of the quality of this paper. Finally, we would like to thank the National Sciences and Engineering Research Council (NSERC) of Canada for financial support.

REFERENCES

Chené, A.-N 2007, Ph.D. Thesis, Université de Montréal

Chené, A.-N, & St-Louis, N., 2009a, in preparation

Chené, A.-N, & St-Louis, N., 2009b, in preparation

Cranmer, S. R., & Owocki, S. P. 1996, ApJ, 462, 469

Dessart, L., & Chesneau, O. 2002, A&A, 395, 209

Dessart, L., & Owocki, S. P. 2002a, A&A, 383, 1113

Dessart, L., & Owocki, S. P. 2002b, A&A, 393, 991

Dessart, L., & Owocki, S. P. 2003, A&A, 406, L1

Dessart, L., & Owocki, S. P. 2005a, A&A, 432, 281

Dessart, L., & Owocki, S. P. 2005b, A&A, 437, 657

Fullerton, A. W., Gies, D. R., & Bolton, C. T. 1996, ApJS, 103, 475

Hackwell, J. A., Gehrz, R. D., Smith, J. R., & Strecker, D. W. 1976, ApJ, 210, 137

Hamann, W.-R., Schmutz, W., & Wessolowski, U. 1988, A&A, 194, 190

Hamann, W.-R., Gräfener, G., & Liermann, A. 2006, A&A, 457, 1015

Hamann, W.-R., & Gräfener, G. 2007, Massive Stars in Interactive Binaries, 367, 141

Hamann, W.-R., Koesterke, L., & Wessolowski, U. 1995, A&A, 299, 151

Heger, A., & Langer, N. 2000, ApJ, 544, 1016

Heger, A., Langer, N. & Woosley, S.E. 2000, ApJ,528, 368

Heger, A., Woosley, S. E., & Spruit, H. C. 2005, ApJ, 626, 350

Herrero, A., Kudritzki, R.P., Vilchez, J.M., Kunze,D., Butler, K., & Haser, S. 1992, A&A, 261, 209

Hill, G. M., Moffat, A. F. J., St-Louis, N. & Bartzakos, P. 2000, MNRAS, 318, 402

Hirschi, R., Meynet, G., & Maeder, A. 2004, A&A, 425, 649

Howarth, I.D., Siebert, K.W., Hussain, G.A.J. & Prinja, R.K. 1997, MNRAS, 284, 265

Howarth, I.D. 2004, in *Stellar Rotation*, Proc. of in IAU Symp. 215, eds. A. Maeder & P. Eenens, San Francisco: ASP, 33

Howarth, I. D., & Prinja, R. K. 1989, ApJS, 69, 527

Howarth, I. D., & Schmutz, W. 1992, A&A, 261, 503

van der Hucht K.A. 2001, New Astronomy Review, 45, 135

Hundhausen, A. J. 1972, Solar Wind, 393

Langer, N. 1992, A&A, 265, L17

Langer, N. & Maeder, A. 1995, A&A, 295, 685

Lépine, S., Moffat, A. F. J., & Henriksen, R. N. 1996, ApJ, 466, 392

Lépine, S.& Moffat, A. F. J., 1999, ApJ, 514, 909

MacFadyen, A. I., & Woosley, S. E. 1999, ApJ, 524, 262

MacFadyen, A. I., Woosley, S. E., & Heger, A. 2001, ApJ, 550, 410

Maeder, A. 1987, A&A, 178, 159

Marchenko, S.V., Moffat, A.F.J., Eversberg, T., Hill, G.M., Tovmassian, G.H., Morel, T., & Seggewiss, W. 1998, MNRAS, 294, 642

Massey, P. 1980, ApJ, 236, 526

Massey, P., & Conti, P. S. 1981, ApJ, 244, 173

McCandliss, S. R., Bohannan, B., Robert, C., & Moffat, A. F. J. 1994, Ap&SS, 221, 155

Meynet, G., Maeder, A., Schaller, G., Schaerer, D., & Charbonnel, C. 1994, Astron. Astrophys. Suppl., 103, 97

Meynet, G.& Maeder, A. 2000, A&A, 361, 101

Meynet, G.& Maeder, A. 2003, A&A, 404, 975

Moffat, A. F. J., Drissen, L., Lamontagne, R., & Robert, C. 1988, ApJ, 334, 1038

Morel, T., St-Louis, N., & Marchenko, S. V. 1997, ApJ, 482, 470

Morel, T., et al. 1999, ApJ, 518, 428

Morel, T., Marchenko, S.V., Pati, A.K., Kuppuswamy, K., Carini, M.T., Wood, E. & Zimmerman, R. 2004, MNRAS, 351, 552

Owocki, S. P., Castor, J. I., & Rybicki, G. B. 1988, ApJ, 335, 914

Penny, L.R. 1996, ApJ, 463, 737

Prinja, R. K., Barlow, M. J., & Howarth, I. D. 1990, ApJ, 361, 607

Prinja, R. K., & Smith, L. J. 1992, A&A, 266, 377

Robert, C. 1992, PhD thesis, Université de Montréal

St-Louis, N., Dalton, M. J., Marchenko, S. V., Moffat, A. F. J., & Willis, A. J. 1995, ApJ, 452, L57

Spruit, H. C. 2002, A&A, 381, 923

Williams, P. M., Beattie, D. H., Lee, T. J., Stewart, J. M., & Antonopoulou, E. 1978, MNRAS, 185, 467

Woosley, S. E. 1993, ApJ, 405, 273

Woosley, S.E., Langer, N. & Weaver 1993, ApJ, 411, 823

Woosley, S. E., & Heger, A. 2006, ApJ, 637, 914

Yoon, S.-C., Langer, N., & Norman, C. 2006, A&A, 460, 199

Zubko, V. G. 1993a, A&AT, 3, 131

Zubko, V. G. 1993b, A&AT, 3, 141
